The 2D Ising model and the search for Onsager's phase transition

René Ask, Kaspara Skovli Gåsvær & Maria Linea Horgen
(Dated: November 18, 2019)

In this paper we study the 2-dimensional Ising model to confirm the second order phase transition predicted by L. Onsager [6]. We performed Monte Carlo simulations using the Metropolis algorithm on several finite lattices for a set of temperatures. The measured heat capacity C_V was then interpolated using cubic-spline interpolation. The maxima of these interpolants were fitted with the least squared method using the power law behaviours and critical exponents derived from mean-field theory. We estimated the critical temperature to $T_C = 2.266 \pm 0.003$. The inferred error is likely too small as errors in the data points and the computed interpolants were neglected. We therefore view our results as a preliminary confirmation of the predicted phase transition.

I. INTRODUCTION

The Ising model is a mathematical framework which models a system of spins classically. In the two-dimensional case, the model is shown to exhibit a second order phase transition in the thermodynamic limit, in other words, when $L \to \infty$ for a $L \times L$ lattice. The model exhibits a universal behaviour for phase transitions, whether it be gas, liquid or superconductors, that is to say, one model to describe them all. In fact, it can be applied to a wide variety of binary systems, from neuroscience to socio-economic models.

In this article we'll confine ourselves to the study of phase transitions in a magnetic system for different lattice sizes and temperatures. To simulate this system, we'll perform Monte Carlo (MC) simulations using a special sampling rule known as the *Metropolis* algorithm. To this end, we will first develop a code that reproduces the analytical expressions derived in VII A. We'll then move on to estimate the time it takes to reach equilibrium, known as equilibration time, to intelligibly decide when proper measurements can be performed. Successively, we'll investigate the rate at which proposed spin-configurations are accepted as a consistency check with the physical expectations of the model. As a final test of our implementation, we'll check that the sample distribution produced by the MC simulation is consistent with the expected Boltzmann distribution at carefully chosen temperatures. Next up, we'll parallelize the code with MPI and study a small set of compiler flags to achieve a proper speedup which we'll then use to perform the larger simulations for a set of lattice sizes and temperatures in which we expect the critical temperature to reside. We'll specifically measure the heat capacity of the system (among other thermodynamic quantities), and use the maxima of these measurements on the temperature interval to estimate the critical temperature T_C as $L \to \infty$. This is done by application of the power law behaviour (proportionality relations derived by mean-field theory) the model exhibits [4].

For codes and their documentation, see [1].

II. FORMALISM

A. The 2D Ising Model

The 2-dimensional Ising model for a square lattice in the absence of an external magnetic field is modelled as

$$H = -J \sum_{\langle ij \rangle} s_i s_j, \tag{1}$$

where H is the total energy of the system, J is coupling constant taken to be the same for every spin site and the sum describes the spin-spin interaction between nearest neighbours. The spins can assume values $s_i = \pm 1$, corresponding to spin up or spin down, respectively. The model assumes that the system of spins is in contact with a reservoir (also known as a thermal bath) with temperature T.

In this article, we'll use natural units such that $k_B = J = 1$, where k_B is the Boltzmann constant.

1. *Benchmarking the code*

The two dimensional Ising model has analytical solutions to several thermodynamic quantities and hence their expectation values as long as the external magnetic field is zero. The expectation values of interest are the mean energy $\langle E \rangle$, the mean absolute value of the magnetic moment $\langle |M| \rangle$ (which we'll refer to as mean magnetization), the heat capacity C_V and the magnetic susceptibility χ. To ensure our implemented codes works properly, we'll compare them with the analytical values for the expectation values listed above as functions of temperature T using periodic boundary conditions for $L = 2$. The closed-form expressions are listed in section VII A.

B. Phase Transitions

The 2D Ising model is known to display a phase transition in the limit $L \to \infty$. The critical temperature T_C

at which this phase transition happens is shown to be [6]

$$T_C = \frac{2J}{\ln\left(1+\sqrt{2}\right)} \simeq 2.269J. \tag{2}$$

For temperatures below T_C, the system exhibits what is called a *ferromagnetic phase* where it possesses a spontaneous magnetization because the spins tend to align with each others in the absence of an external magnetic field, yielding $|m| = 1$ in the limit $T \to 0$, where $|m|$ is the net magnetization per spin. Above this temperature, the system is in a *paramagnetic phase* because the average magnetization will be zero in the absence of an external magnetic field.

The critical temperature obeys the following relation [3]:

$$T_C(L) = \frac{1}{L} + T_C(\infty), \tag{3}$$

where $T_C(L)$ is the critical temperature found on a finite lattice with lattice size $L \times L$. From eq. (3) we will estimate T_C by calculating the heat capacity C_V for $L \in \{40, 60, 80, 100\}$ and $T \in [2.0, 2.4]$ with step size $\Delta T = 10^{-3}$. When $L \to \infty$ and $T \to T_C$, the heat capacity diverges such that $C_V \to \infty$. Hence, to estimate $T_C(L)$ for a finite L, we'll read off the maxima of $C_V(T, L)$ and combine this with eq. (3) to estimate $T_C(\infty)$. This is done using the standard least squares method. The following sections of the formalism is based on the treatment found here [5].

C. Preliminaries - statistical physics

Suppose we choose M spin states μ. Then the *estimator* Q_M of a real observable Q is defined as

$$Q_M \equiv \frac{\sum_\mu Q_\mu e^{-\beta E_\mu}/p_\mu}{\sum_\nu e^{-\beta E_\nu}/p_\nu}, \tag{4}$$

where both summations run of the same M states and p_μ is some probability distribution (PDF). The estimator has the property

$$\lim_{M\to\infty} Q_M = \langle Q \rangle, \tag{5}$$

where $\langle Q \rangle$ is the expectation value of the observable Q defined as

$$\langle Q \rangle = \frac{1}{Z}\sum_\mu Q_\mu e^{-\beta E_\mu}, \tag{6}$$

and Z is the partition function

$$Z = \sum_\mu e^{-\beta E_\mu}. \tag{7}$$

D. Importance sampling

For a large system, computing $\langle Q \rangle$ is usually intractable, simply because the number of possible microstates for the 2D Ising model is 2^{L^2}, which makes it computationally expensive to compute the partition function. We must therefore resort to some measurement process from which we can extract measured values and compute their estimators. To make this measurement process efficient, however, we cannot sample spins at random, since this will increase the likelihood that the system ends spin states which aren't particularly likely. This will require a large amount of measurements in order for the estimators to converge to the true expectation values. This prompts us to choose the probabilities p_μ such that our simulation tends to end up in macrostates that are more likely such as to minimize the number of necessary measurements. Choosing p_μ to be the Boltzmann distribution

$$p_\mu = \frac{1}{Z}e^{-\beta E_\mu}, \tag{8}$$

is tantamount to saying that we choose a state μ with probability p_μ (though, we do not claim that this is necessarily the *most* efficient choice, just that it is *more* efficient than sampling uniformly). The estimator then reduces to

$$Q_M = \frac{1}{M}\sum_\mu Q_\mu. \tag{9}$$

The rationale for this choice lies in the fact that the system will tend to spend a majority of its time in a small subset of possible states μ, so weighting the states according to how likely they are will more closely correspond to the physical system we're modelling. Putting the physical argument aside, this will also reduce the number of necessary measurements significantly as opposed to sampling uniformly.

E. Heat Capacity and Magnetic Susceptibility

The heat capacity of the system is

$$C_V \equiv \frac{\langle E^2 \rangle - \langle E \rangle^2}{k_B T^2}, \tag{10}$$

and the magnetic susceptibility is defined as

$$\chi \equiv \frac{\langle M^2 \rangle - \langle |M| \rangle^2}{k_B T}, \tag{11}$$

where we use $\langle |M| \rangle$ instead of $\langle M \rangle$.

F. Markov Processes

To model the system, we need some tactful way to sample the states μ. To this end, we shall apply a short list

of principles that makes the sampling process possible. But first, some definitions. A Markov process (or chain) is a scheme which takes a state μ and generates a new state ν with a *transition probability* $P(\mu \to \nu)$, which is the probability that the system will transition from state μ to state ν.

A Markov process must obey a couple of conditions: The first of which is that the transition probabilities are time-independent. The second is that the $P(\mu \to \nu)$ should only depend on the states μ and ν, and thus is independent of the system's time evolution. Furthermore, they must obey

$$\sum_{\nu} P(\mu \to \nu) = 1, \tag{12}$$

which is equivalent to say that the Markov process must put the system in *some* state ν when presented with the state μ. Note that the transition $\mu \to \mu$ is also permitted such that $P(\mu \to \mu) \neq 0$.

1. Ergodicity

The first important principle we must contend with is the condition of *ergodicity* which states that it's possible to reach any state ν from any state μ given a long enough Markov chain. This constraint is important because every state μ in the Boltzmann distribution p_μ has a non-zero probability.

2. Detailed Balance

The second constraint the Markov process must obey is what is known as the condition of *detailed balance*. In particular for our case, this principle states that on average, the system makes the transition $\mu \to \nu$ just as much as the transition $\nu \to \mu$. Mathematically, this statement is

$$p_\mu P(\mu \to \nu) = p_\nu P(\nu \to \mu). \tag{13}$$

Clearly, eq. (13) implies that

$$\frac{P(\mu \to \nu)}{P(\nu \to \mu)} = \frac{p_\nu}{p_\mu} = e^{-\beta(E_\nu - E_\mu)}. \tag{14}$$

If the probability $P(\nu \to \mu)$ rotates around several different values, the Markov process can reach a dynamic equilibrium. This is called a limit cycle and implies that the final state may not be unambiguous. To inhibit this, the condition of detailed balance must be satisfied.

G. Selection probabilities and acceptance ratios

Since its only the ratio $P(\mu \to \nu)/P(\nu \to \mu)$ that matters, we are free to make any change to the two transition probabilities as long as the ratio is unchanged. We can therefore write

$$P(\mu \to \nu) = g(\mu \to \nu)A(\mu \to \nu), \tag{15}$$

where $g(\mu \to \nu)$ is the selection probability which tells us how likely it is that from a given state μ, our process will generate a new target state ν, and $A(\mu \to \nu)$ is the acceptance ratio which encodes information that corresponds to the fraction of time the new target state is to be accepted by our algorithm. The remaining fraction, the system should be left in the initial state it presented with. With this in mind, eq. (14) can be written as

$$\frac{P(\mu \to \nu)}{P(\nu \to \mu)} = \frac{g(\mu \to \nu)A(\mu \to \nu)}{g(\nu \to \mu)A(\nu \to \mu)}. \tag{16}$$

1. The Metropolis Algorithm

The Metropolis algorithm sets $g(\mu \to \nu) = 1/N$ where N is the number of spins in the system, such that

$$\frac{A(\mu \to \nu)}{A(\nu \to \mu)} = e^{-\beta(E_\nu - E_\mu)}. \tag{17}$$

Suppose $E_\nu > E_\mu$. Since it's only the ratio that needs to obey the equality, we can make this algorithm efficient by a simple trick: the largest of the two acceptance ratios is set to 1. Then

$$\frac{A(\mu \to \nu)}{A(\nu \to \mu)} = e^{-\beta(E_\nu - E_\mu)} < 1, \tag{18}$$

where we impose $A(\nu \to \mu) = 1$. In the case $E_\nu < E_\mu$, the energy of the system is lowered, and on grounds that physical systems has a tendency to spontaneously transition from higher to lower energy states, the Metropolis algorithm accept the transition regardless. Thus the acceptance probabilities can be summarized as follows.

$$A(\mu \to \nu) = \begin{cases} e^{-\beta(E_\nu - E_\mu)}, & E_\nu - E_\mu > 0, \\ 1, & \text{else.} \end{cases} \tag{19}$$

H. Single-spin-flip dynamics

In order for the Markov process to generate new states ν from a presented state μ, a new state ν must be constructed and then accepted or rejected according to eq. (19). As stated earlier, the fluctuation in energy tends to be low when the system reaches equilibrium and to model this, we shall apply what is known as *single-spin-flip dynamics*: given as state μ we pick a random spin site (i, j) on the square lattice and flip it (or reject the flip) according to eq. (19). This device ensures that our algorithm does not consider states which implies a large change in energy when the system makes the transition $\mu \to \nu$. This choice also conserves ergodicity since the

system easily can transition back to μ in a reasonable amount of time. At this point, the reasoning behind the choice $g(\mu \to \nu) = 1/N$ also becomes clear. By restricting ourselves to a single spin-flip, there are exactly N spins to flip and thus N accessible states ν to which the system can transition into if we include the initial state μ.

We will collect the number of accepted spin-flips and perform an analysis of it as a function of MC cycles to see how the quantity behaves on two specific temperatures specifically for $T = 1.0$ and $T = 2.4$, corresponding to the system in its two different phases: the ferro- and paramagnetic phase, respectively.

I. Change in energy and magnetization by a spin-flip

When a spin of the system is flipped, it becomes necessary to compute the change in energy and magnetization of the system during the Markov chain. Assume the system is in the spin state μ and we're to consider a transition $\mu \to \nu$ of the system, and suppose the spin we flip is located on spin site k. The change in energy is then only dependent upon the four neighbours of the spin at site k, since all other spins are unchanged. Furthermore, since the nearest neighbours of site k is unchanged, $s_i^\nu = s_i^\mu$ for these spins and thus

$$\begin{aligned} \Delta E &\equiv E_\nu - E_\mu \\ &= -J \sum_{\langle ij \rangle} s_i^\nu s_j^\nu + J \sum_{\langle ij \rangle} s_i^\mu s_j^\mu \\ &= -J \sum_{\langle ik \rangle} s_i^\nu (s_k^\nu - s_k^\mu), \end{aligned} \tag{20}$$

where the sum runs over the nearest neighbours of a specific spin site k. We can simplify this term further. If $s_k^\mu = 1$, then flipping it yields $s_k^\nu = -1$. This means that $s_k^\nu - s_k^\mu = -2$. Similarly, if $s_k^\mu = -1$, a flip gives $s_k^\nu = 1$ and thus $s_k^\nu - s_k^\mu = 2$. Therefore, the change in energy can be computed as

$$\Delta E = 2J s_k^\mu \sum_{\langle ik \rangle} s_i^\mu \tag{21}$$

The change in the magnetization by the transition $\mu \to \nu$ is far simpler to compute. Since only the spin at site k is changed, the change is given by

$$\begin{aligned} \Delta M &\equiv M_\nu - M_\mu \\ &= \sum_i s_i^\nu - \sum_j s_j^\mu \\ &= s_k^\nu - s_k^\mu \\ &= 2 s_k^\nu \end{aligned} \tag{22}$$

J. Equilibration time

To determine the equilibration time τ_{eq}, we shall for each a few temperatures T study the behaviour of estimators Q_M over time measured in number of lattice sweeps which is defined as the number of MC cycles per spin. To increase the likelihood that the equilibrium the system settles into is not some local minima, we shall do this starting from two distinct initial states. The first state is the equilibrium state for $T = 0$ in which the system is in one of the ground states, meaning that all of the spins is either spin up or spin down. The second is an equilibrium state for $T = \infty$ for which all the spins are randomly oriented since there's an infinite amount of energy available to flip the spins at random, and thus no particular ordering of the spins are preferred.

III. ALGORITHMS

To summarize the formalism of the preceding section, we write up the main algorithm of our code as follows.

Algorithm 1 MC simulation with Metropolis sampling

```
Pick T, μ.                                   ▷ Temperature and initial spin
Compute E_μ                                  ▷ Initial energy
for k = 1, 2, ..., N do                      ▷ Loop over MC samples
    Sample i, j ∈ [0, L − 1] ∩ ℤ             ▷ Random numbers
    Compute ΔE                               ▷ ΔE of μ → ν
    if ΔE < 0 or r < e^{−βΔE} then           ▷ r ∈ (0, 1) from RNG
        μ → ν                                ▷ Accept flip
        E = E + ΔE                           ▷ Update energy
        M = M + ΔM                           ▷ Update magnetization
    else
        μ → μ                                ▷ Reject flip
    ⟨E⟩ = ⟨E⟩ + E                            ▷ Add contribution to mean
    ⟨|M|⟩ = ⟨|M|⟩ + M                        ▷ Add contribution to mean
Compute estimators
```

IV. RESULTS

A. The $L = 2$ case

Table I and II presents a number of selected expectation values for the energy, mean absolute magnetization, heat capacity and magnetic susceptibility. The values in table I corresponds with an ordered initial spin configuration, and table II with a random configuration. From the tables it is evident that the selected expectation values converges to the analytical values.

B. Estimation of equilibration time

We ran our code to produce an estimate of the equilibration time on a system with $L = 20$. FIG. 1 shows

$\log_{10}(t)$	$\langle E\rangle/L^2$	$\langle\lvert M\rvert\rangle/L^2$	C_v/L^2	χ/L^2
3.0	-1.988000	0.996125	0.099424	0.011190
4.0	-1.996700	0.998950	0.026756	0.002996
5.0	-1.995940	0.998650	0.032454	0.004033
∞	-1.995982	0.998660	0.032082	0.004011

TABLE I. The table shows computed thermodynamic quantities for several times t measured in Monte Carlo samples per spin with $L = 2$ and $T = 1$, starting from an ordered spin configuration. The row with $\log_{10}(t) = \infty$ denotes the analytical values.

$\log_{10}(t)$	$\langle E\rangle/L^2$	$\langle\lvert M\rvert\rangle/L^2$	C_v/L^2	χ/L^2
3.0	-1.997000	0.999000	0.023964	0.002996
4.0	-1.997100	0.999050	0.023166	0.002796
5.0	-1.995915	0.998631	0.032693	0.004125
∞	-1.995982	0.998660	0.032082	0.004011

TABLE II. The table shows computed thermodynamic quantities for several times t measured in Monte Carlo samples per spin with $L = 2$ and $T = 1$, starting from a random spin configuration. The row with $\log_{10}(t) = \infty$ denotes the analytical values.

the energy of the system as a function of time measured in Monte Carlo cycles per spin, where the system was initially in a ground state spin state with $T = 1.0$. We observe that in this case, equilibrium is reached almost instantaneously.

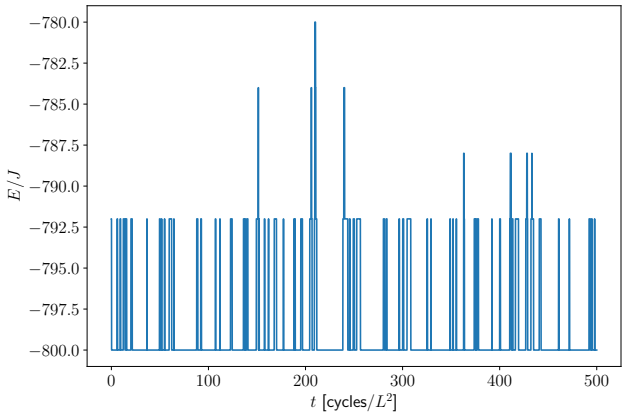

FIG. 1. The figure shows the energy E/J of the system as a function of time measured in Monte Carlo cycles per spin with $T = 1$ and $L = 20$. The simulation was started from an initial $T = 0$ spin state. Note that equilibrium is reached roughly instantaneously in this case.

We kept the initial spin state as the trivial ground state and changed the temperature to $T = 2.4$, which produced the results shown in FIG. 2. Here too, the system had a size of $L = 20$. For these parameters equilibrium was reached around $t = 1000$.

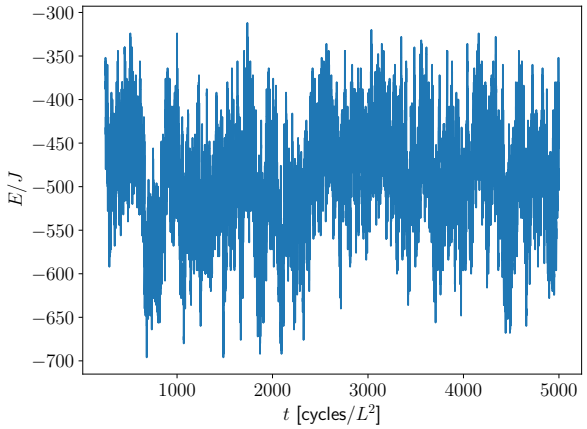

FIG. 2. The figure displays the energy E/J of the system as a function of time measured in Monte Carlo cycles per spin with $T = 2.4$ and $L = 20$. The simulation was started from an initial $T = 0$ spin state. In this case, equilibrium is reached in about $t = 1000$.

FIG. 3 shows the mean energy per spin, $\langle E\rangle/L^2$, as a function of time t measured in Monte Carlo samples per spin for both a ground state initiation and a random initiation with $T = 1.0$.

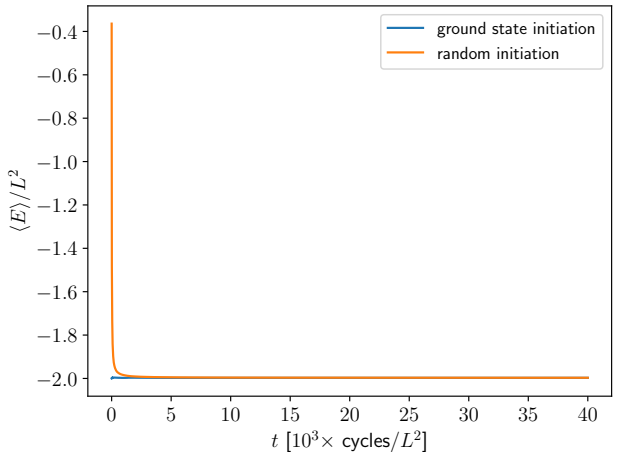

FIG. 3. The figure shows the mean energy per spin, $\langle E\rangle/L^2$, as a function of time t measured in Monte Carlo samples per spin with $T = 1.0$ and $L = 20$. It's clear that both simulations converge to same value.

The mean magnetization per spin, $\langle\lvert M\rvert\rangle/L^2$, as a function of time t measured in Monte Carlo samples per spin with $T = 1.0$, is presented in FIG. 4.

FIG. 5 shows the mean energy per spin, $\langle E\rangle/L^2$, as a function of time t measured in Monte Carlo samples per spin for both a ground state initiation and a random initial spin state with $T = 2.4$.

The mean magnetization per spin, $\langle\lvert M\rvert\rangle/L^2$, as a

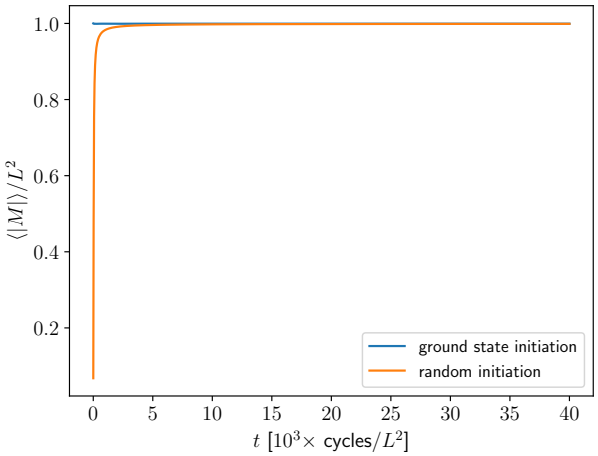

FIG. 4. The figure shows the mean magnetization per spin, $\langle |M| \rangle / L^2$, as a function of time t measured in Monte Carlo samples per spin with $T = 1.0$ and $L = 20$. Observe that both simulations approach the same value.

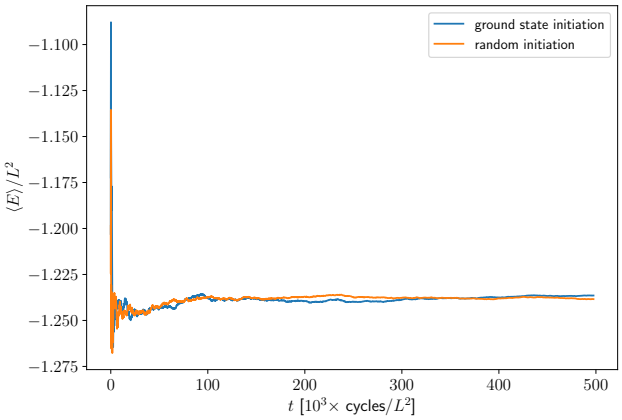

FIG. 5. The figure exhibit the mean energy per spin, $\langle E \rangle / L^2$, as a function of time t measured in Monte Carlo samples per spin with temperature $T = 2.4$ and $L = 20$. Evidently, they approach the same minimum as time becomes fairly large.

function of time t measured in Monte Carlo samples per spin with $T = 2.4$, for both a random spin initiation and ground state initiation, is shown in FIG. 6.

C. Accepted spin-flips

FIG. 7 and 8 presents the number of accepted spin-flips for $T = 1.0$ and $T = 2.4$, with $L = 20$. Note that the measurements were made without a burn-in period.

We observe that number of accepted spin-flips is approximately 300 times higher in the $T = 2.4$ case.

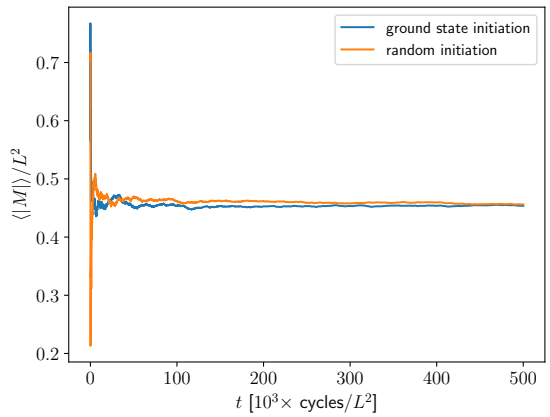

FIG. 6. The figure shows the mean magnetization per spin, $\langle |M| \rangle / L^2$, as a function of time t measured in number of Monte Carlo samples per spin for temperature $T = 2.4$ and $L = 20$. Observe that they converge towards the same minimum.

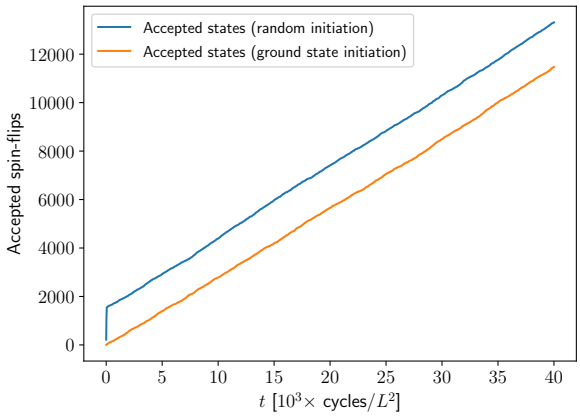

FIG. 7. The figure displays the number of accepted spin-flips as a function of time t measured in MC samples per spin with $T = 1.0$, with $L = 20$.

D. The sample distribution of the energy

The (normalized) measured probability distributions $P(E)$ for a lattice of size $L = 20$ with temperatures $T = 1.0$ and $T = 2.4$ are shown in FIG. 9 and 10. The results in this section were generated with a burn-in period of $\tau_{\text{eq}} = 2500$ and a total simulation time of $t = 10^5$.

FIG. 9 shows the distribution of energies for $T = 1.0$. In this case, the most likely energy is $E/J = -800$. The distribution of energies for $T = 2.4$ is presented in FIG. 10, with a mean value around $E/J = -480$.

Table III lists the computed standard deviations (STDs) of the energy, σ_E, for both the $T = 0$ and $T = \infty$ spin initiations.

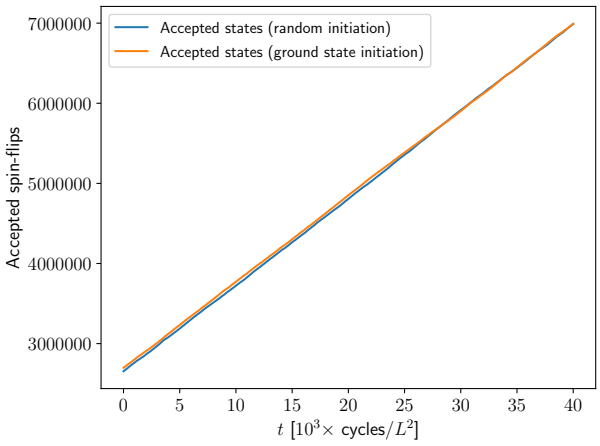

FIG. 8. The figure shows the number of accepted spin-flips as a function of time t measured in MC samples per spin with temperature $T = 2.4$, with $L = 20$.

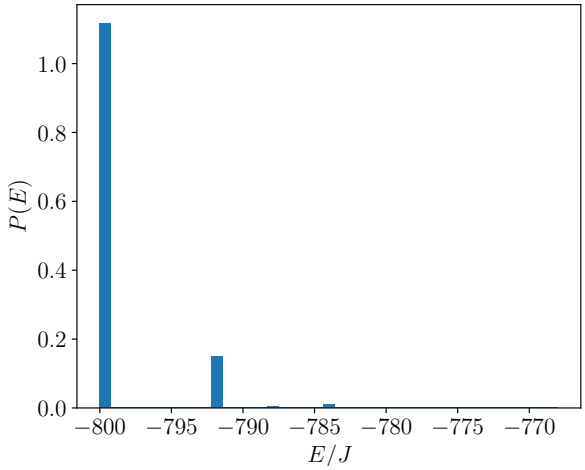

FIG. 9. The figure shows the distribution of energies for $T = 1.0$. We note that the most likely energy state is $E/J = -800$.

T	σ_E (ground state initiation)	σ_E (random initiation)
1.0	2.9868	3.1125
2.4	59.953	55.456

TABLE III. The table presents the computed standard deviations of the energy σ_E from both $T = 0$ and $T = \infty$ spin initiation. These values were computed using a burn-in period of $\tau_{\text{eq}} = 2500$ and a total simulation time of $t = 10^5$.

E. Code optimization

In order to optimize our code, we tested a selection of compiler flags by running the parallelized code with $p = 2$ processes for set of Monte Carlo samples using three different compiler flag options: -O2, -O3 and -Ofast. To

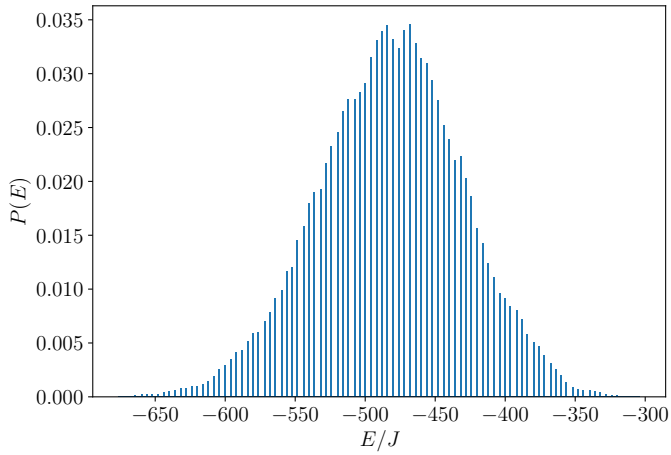

FIG. 10. The figure shows the distribution of energies for $T = 2.4$. We observe from the plot that the probability of energy states is similar to a Gaussian distribution with a mean value around $E/J = -480$.

check that the parallized code achieved a speedup relative to no parallelization, we ran the code with $p = 1$ and $p = 2$ processes. The results are presented in figure 11, where CPU-time is depicted as a function of number of Monte Carlo cycles.

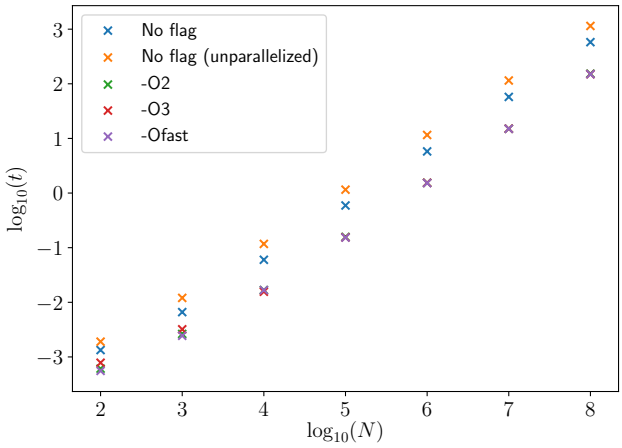

FIG. 11. The figure shows the amount of CPU time spent by the code when using different compiler flags for a set of Monte Carlo cycles. N and t represents Monte Carlo cycles and CPU time, respectively. We used $p = 2$ processors in parallel and a lattice of size $L = 20$. For large values of Monte Carlo cycles we observe that the flags -O2, -O3 and -Ofast exhibit a similar performance.

F. Thermodynamic quantities as a function of temperature

The results in this section was computed using a burn-in period of $\tau_{\text{eq}} = 100$ and a total simulation time $t = 10^6$, measured in Monte Carlo cycles per spin. We used a $T = \infty$ spin state as our initial state. The results are based on 400 temperatures $T \in [2.0, 2.4]$ for all $L \in \{40, 60, 80, 100\}$.

FIG. 12(a) shows the mean energy per spin $\langle E \rangle / L^2$, and FIG. 12(b) displays the mean magnetization per spin $\langle |M| \rangle / L^2$ as functions of temperature T. FIG. 13(a) depicts the magnetic susceptibility per spin.

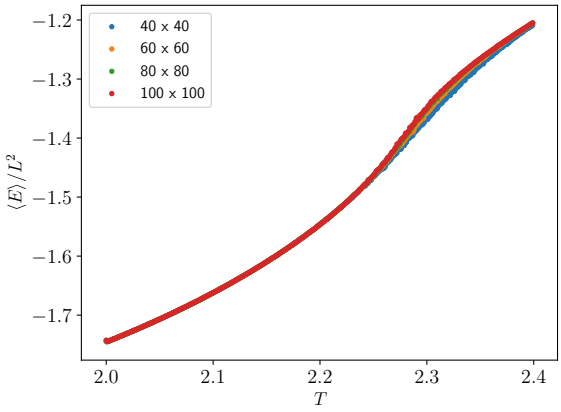

(a)

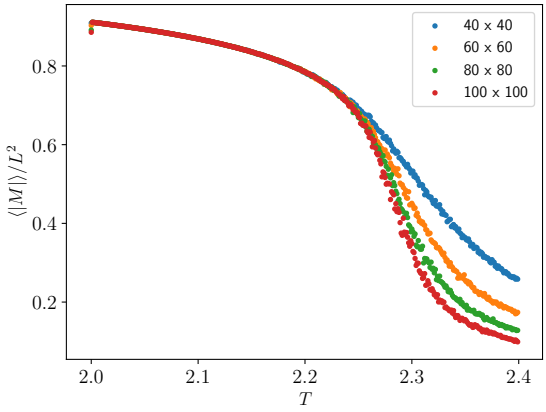

(b)

FIG. 12. The mean values are shown as functions of temperature T for $L \in \{40, 60, 80, 100\}$. The burn-in period was set to $\tau_{\text{eq}} = 100$ with total simulation time of $t = 10^6$ for each L.
(a): The figure shows the mean energy per spin $\langle E \rangle / L^2$.
(b): The figure displays the mean magnetization per spin $\langle |M| \rangle / L^2$.

From the data points of C_V/L^2, shown in FIG. 13(b), we created four interpolants to fit the data using scipy's interpolation library, see [2] for documentation. The result is shown in FIG. 14(a)

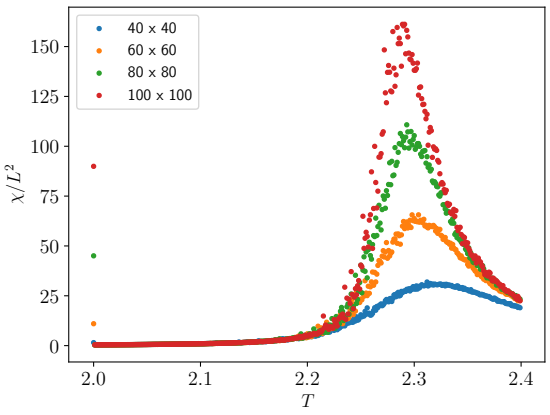

(a)

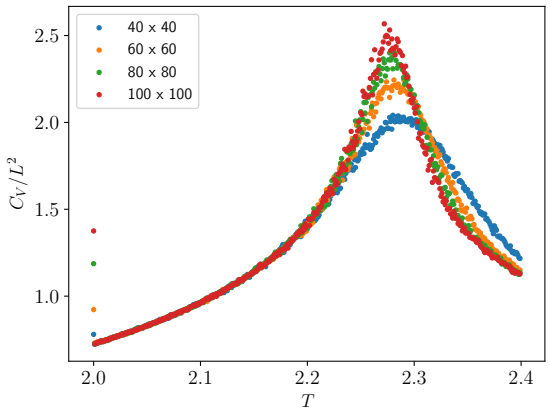

(b)

FIG. 13. The measured observables are shown as functions of temperature T for $L \in \{40, 60, 80, 100\}$. The burn-in period was set to $\tau_{\text{eq}} = 100$ with total simulation time of $t = 10^6$ for each L.
(a): The figure shows the magnetic susceptibility per spin χ/L^2.
(b): The figure depicts the computed heat capacity per spin C_V/L^2.

We measured the maximum of each interpolant and fitted the data points according to eq. (3) using the least squares method. The fitted function is shown in FIG. 14(b) from which we obtained the following estimate of the critical temperature in the limit $L \to \infty$.

$$T_C(\infty) = 2.266 \pm 0.003. \tag{23}$$

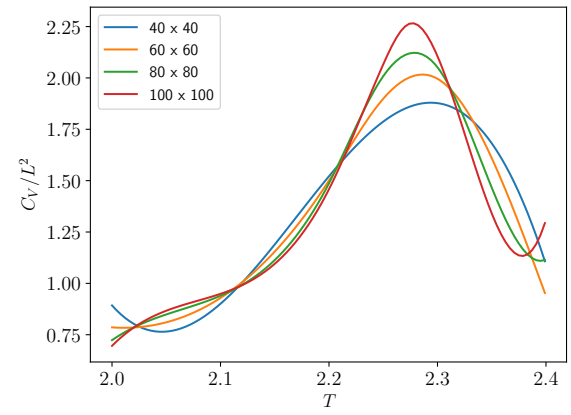

(a)

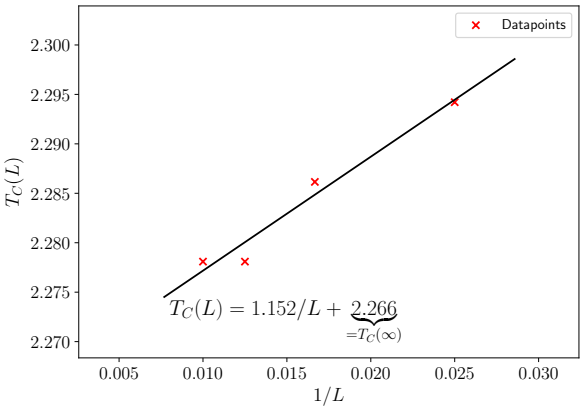

(b)

FIG. 14. **(a)**: The figure shows C_V/L^2 obtained through cubic-spline interpolation with smoothing as a function of temperature T for $L \in \{40, 60, 80, 100\}$.
(b): The figure displays a least-squares fit of $T_C(L)$ as a function of $1/L$ to data points $(L^{-1}, T_C(L))$ obtained from the interpolants in FIG. 14(a) by finding the maximum of each interpolant.

V. DISCUSSION

A. Agreement in the $L = 2$ case

From table I and II, we observe that our simulation achieved a reasonable agreement with the analytical values for $T = 1.0$, demonstrating that our code works with the $L = 2$ case.

B. The estimated equilibration time

It's clear from FIG. 1 that equilibrium is reached almost instantaneously in the case with $T = 1.0$. For the case with $T = 2.4$ we achieved roughly an equilibration time of $t = 1000$, as usual, measured in MC cycles per spin. Both results was obtained with the initial $T = 0$ spin state, which explains the difference in equilibration time for the two temperatures for the following reason: the $T = 0$ spin state lies closer to the subset of spin states the system will converge to in the case of $T = 1$ as opposed to $T = 2.4$. This is why the equilibration time in the latter case is longer than the former.

Naturally, the larger simulations for $T \in [2.0, 2.4]$ should've, ideally, been run with a burn-in period corresponding to the latter result in order to increase the likelihood that the system already reached thermodynamic equilibrium before measurements were made. However, we chose to initiate the system from a $T = \infty$ state as this were likely to reduce the equilibration time somewhat, which is why we ran the code with a burn-in period of $\tau_{\text{eq}} = 100$ instead. This could then give us more measurements for a given total simulation time and hopefully then give us less variance in the end results which ostensibly is consistent with FIG. 12(a) and 12(b). The point is that some of the initial measurements may be contaminated in the sense that certain measurement values are over-represented with respect to the true probability distribution for a given T. This is a potential systematic error which is difficult to quantify.

C. Accepted spin-flip configurations

As shown in FIG. 7 and 8, the number of accepted spin-flips increases in a linear fashion as time evolves. Though, there's a rapid rate of accepted states around $t = 0$ in FIG. 7 which are likely to arise as a result of the random initiation of spins, which yields a higher initial energy than the $T = 0$ spin state. Thus the Metropolis sampling rule accepts most proposed spin configurations since most of them are likely to decrease the energy of the system. The fact that the number of accepted spin-flips is roughly 300 times higher when $T = 2.4$ is expected considering that the number of accessible energy states increases with temperature.

D. The sample distribution of the energy and measured standard deviation

The probabilities in FIG. 9 and 10 were computed after the steady state was reached, meaning that the initial spin configuration should have been irrelevant when computing the sample distributions of the energy and the STDs. From table III there is a small discrepancy in σ_E for the two initial spin configurations, which we attribute to an insufficient number of measurements.

For the $T = 1$ case the probability for being in the ground state is roughly 97%, which is also reflected through the obtained STD. Here the STD is considered a quantitative measurement of the spread in the data set. As mentioned in the preceding section, the number of ac-

cessible energy states increases with the temperature, so a higher temperature, here $T = 2.4$, yields a larger number of accessible energy states and hence a larger spread. The behaviour observed is thus in agreement with the theory.

E. Speedup by parallelization and optimal choice compiler flags

We studied the optimal choice of compiler flags to use with the larger simulations. Ostensibly, by inspecting FIG. 11, the compiler flags -O2, -O3 and -Ofast produces roughly the same simulation time for large N and thus none of them are preferred over any of the others based solely on time considerations. From the same figure, we note that by elimination of compiler flags, the parallelized code with $p = 2$ processes is faster than the unparallelized one, and thus we achieve a speedup using the parallelization. This suggested that the larger simulations should be run with one of the three mentioned compiler flags and parallelization.

F. The estimate of the critical temperature in the thermodynamic limit

Our estimate on the critical temperature T_C in the thermodynamic limit as given in eq. (23) found from the least squares fit shown in FIG. 14(b). The computed value is in agreement with the analytical value in eq. (2). The computed error, however, is likely to be a little too small since it's the standard deviation obtained from the least squares fit of the maximum values of the interpolants alone. This means that the error due to interpolating the measured values is not taken into account nor is the error in the measurements themselves. Therefore, we consider our result a preliminary result that confirms the existence of the theoretical phase transition in the thermodynamic limit and conclude that this warrants larger, more precise simulations that minimizes the error to achieve a better agreement with the analytical value.

The critical temperature could also have been obtained from the magnetic susceptibility data. So an improvement to the error estimate could have been reached through interpolating both FIG. 13(a) and 13(b), and computing the mean value of the maxima.

VI. CONCLUSION

In this paper we've studied the Ising model in 2-dimensions with the purpose of confirming the theoretically predicted second order phase transition derived by L. Onsager in [6]. This was done by performing Monte Carlo simulations using the Metropolis sampling algorithm to make measurements of thermodynamic quantities for several temperatures and lattice sizes. These measurements were used to compute interpolants for C_V whose maxima were fitted by the least-squares method. This gave an estimate of the critical temperature to be $T_C = 2.266 \pm 0.003$. We view this only as a confirmation of the predicted phase transition. This is due to the error estimate likely being too small because we neglected the error in the measurements and the interpolants when computing the error.

VII. APPENDIX

A. Analytical expressions for a simple 2×2 lattice with periodic boundary conditions

Below follows the analytical calculations for the partition function and the corresponding expectations values for the energy E, the mean absolute value of the magnetic moment or mean magnetization $|M|$, the heat capacity C_V and the susceptibility χ as functions of temperature using periodic boundary conditions. Table IV list the energy and magnetization values for the different spin configurations, as well as their degeneracy. The analytical expectation values are calculated from these values.

$N_\uparrow$	Degeneracy	E	M
4	1	-8J	4
3	4	0	2
2	4	0	0
2	2	8J	0
1	4	0	-2
0	1	-8J	-4

TABLE IV. The table displays the energy, magnetization and degeneracy for the various spin configurations for a two-dimensional system consisting of two spins, where $N_\uparrow$ is the number of spins up. See [4] for a gentle walk through of the calculations.

For simplicity we list the physical quantities of interest below.

$$Z = \sum_i e^{-E_i\beta} = 12 + 2e^{8\beta} + 2e^{-8\beta} = 4(3 + \cosh 8\beta), \qquad \text{where } \beta = (k_B T)^{-1}, \tag{24}$$

$$\langle E \rangle = \sum_i E_i \frac{e^{-E_i\beta}}{Z} = 2\left(-8\frac{e^{8\beta}}{Z}\right) + 2\left(8\frac{e^{-8\beta}}{Z}\right) = -\frac{16}{Z}\left(e^{x} - e^{-x}\right) = -\frac{32}{Z}\sinh 8\beta, \tag{25}$$

$$\left\langle E^2 \right\rangle = \sum_i E_i^2 \frac{e^{-E_i\beta}}{Z} = 2\left(64\frac{e^{8\beta}}{Z}\right) + 2\left(64\frac{e^{-8\beta}}{Z}\right) = \frac{256}{Z}\cosh 8\beta, \tag{26}$$

$$\langle |M| \rangle = \sum_i |M_i| \frac{e^{-E_i\beta}}{Z} = 2\left(\frac{4}{Z}e^{8\beta}\right) + 8\left(\frac{2}{Z}\right) = \frac{8}{Z}\left(e^{8\beta} + 2\right), \tag{27}$$

$$\langle M \rangle = \sum_i |M_i| \frac{e^{-E_i\beta}}{Z} = 0, \tag{28}$$

$$\left\langle M^2 \right\rangle = \sum_i M_i^2 \frac{e^{-E_i\beta}}{Z} = 2\left(16\frac{e^{8\beta}}{Z}\right) + 8\left(\frac{4}{Z}\right) = \frac{32}{Z}\left(e^{8\beta} + 1\right). \tag{29}$$

$$\tag{30}$$

From eq. (10), the heat capacity of the system is

$$C_V = \left[\frac{256}{Z}\cosh 8\beta - \left(-\frac{32}{Z}\sinh 8\beta\right)^2\right]\frac{1}{k_B T^2} = \left[\frac{256}{Z}\left(\cosh 8\beta - \frac{4}{Z}\sinh^2 8\beta\right)\right]\frac{1}{k_B T^2}. \tag{31}$$

while the magnetic susceptibility, from eq. (11), can be expressed as

$$\chi = \left[\left(16\frac{e^{8\beta}}{Z}\right) + 4\left(\frac{4}{Z}\right) + 4\left(\frac{4}{Z}\right) + \left(16\frac{e^{8\beta}}{Z}\right) - 0\right]\beta = \frac{32}{Z}\left(e^{8\beta} + 1\right)\beta. \tag{32}$$

---

[1] Link to our Github repository with code documentation. https://github.com/reneaas/ComputationalPhysics/tree/master/projects/project4.

[2] Specifically, Univariatespline were used. https://docs.scipy.org/doc/scipy/reference/generated/scipy.interpolate.UnivariateSpline.html.

[3] Morten Hjorth-Jensen. Project 4, computational physics - fys3150. https://github.com/CompPhysics/ComputationalPhysics/blob/master/doc/Projects/2019/Project4/pdf/Project4.pdf.

[4] Morten Hjorth-Jensen. *Computational Physics, Lecture Notes Fall 2015*, chapter 13.3-13.4. 2015.

[5] M. E. J. Newman and G. T. Barkema. *Monte Carlo Methods in Statistical Physics*, chapter 2-3. Oxford University Press, 1999.

[6] Lars Onsager. Crystal statistics. i. a two-dimensional model with an order-disorder transition. *Phys. Rev. 65, 117*, 1944.